HHS Public Access

Author manuscript

Cancer Sci. Author manuscript; available in PMC 2016 April 01.

Published in final edited form as:

Cancer Sci. 2015 April ; 106(4): 421–429. doi:10.1111/cas.12610.

Identification of a novel E-box binding PI polyamide inhibiting MYC-driven cell-proliferation

Rajeev Mishra[1,3], **Takayoshi Watanabe**[1,2], **Makoto T. Kimura**[1], **Nobuko Koshikawa**[2], **Maki Ikeda**[1], **Shota Uekusa**[1], **Hiroyuki Kawashima**[1,7], **Xaofei Wang**[1], **Jun Igarashi**[1], **Diptiman Choudhury**[3], **Carla Grandori**[4], **Christopher J. Kemp**[4], **Miki Ohira**[2], **Narendra Kumar Verma**[5], **Yujin Kobayashi**[6], **Jin Takeuchi**[6], **Tsugumichi Koshinaga**[7], **Norimichi Nemoto**[8], **Noboru Fukuda**[9], **Masayoshi Soma**[10], **Takeshi Kusafuka**[7], **Kyoko Fujiwara**[10], and **Hiroki Nagase**[1,2,*]

[1]Division of Cancer Genetics, Department of Advanced Medical Science, Nihon University Research Institute of Medical Science, Tokyo 173-8610, Japan

[2]Chiba Cancer Center Research Institute, 666-2 Nitona-cho, Chuo-ku, Chiba-shi, Chiba 260-8717

[3]Department of Medicine, Cedars-Sinai Medical Center, Samuel Oschin Comprehensive Cancer Institute, Los Angeles, CA, USA

[4]Divisions of Human Biology, Fred Hutchinson Cancer Research Center, Seattle, Washington 98109, USA

[5]Department of Biological Sciences, Padova University 35121 Italy

[6]Division of Hematology, Department of Internal Medicine, Nihon University Research Institute of Medical Science, Tokyo 173-8610, Japan

[7]Division of Pediatric Surgery, Department of Surgery, Nihon University Research Institute of Medical Science, Tokyo 173-8610, Japan

[8]Department of Pathology and Microbiology, Nihon University Research Institute of Medical Science, Tokyo 173-8610, Japan

[*]**Corresponding Author:** Dr Hiroki Nagase, Chiba Cancer Center Research Institute, 666-2 Nitona-cho, Chuo-ku, Chiba 260-8717, Japan. Tel: 81-43-264-5431, Fax: 81-43-263-8175, hnagase@chiba-cc.jp.

Disclosure of potential conflict of interest

The authors have no conflict of interest.

Supporting Information:

Doc. S1. Supplementary Materials and Methods

Fig. S1. Anti-proliferative effect of Myc-5.

Fig. S2. Myc-5 localizes into nucleus.

Fig. S3. In vivo binding of Myc-5 at CDK4 gene promoter.

Fig. S4. Heat map represents the functional annotated transcripts that are identified by unpaired two-class significance analysis of microarray (SAM) analysis with a false discovery rate (FDR) of 0% from cells treated with DMSO (Control), Mismatch polyamide and Myc-5.

Table S1. List of FITC-labeled oligomer sequence designed for EMSA.

Table S2. List of primers used in quantitative reverse transcription PCR.

Table S3. List of primer used for Chromatin immunoprecipitation (ChIP) real-time PCR.

Table S4. List of the promoter-associated E-boxes genes.

Table S5. Kinetic constant for Myc-5 PI polyamide and mismatch binding.

Doc. S2. Reference List

[9]Life Science, Advanced Research Institute for the Sciences and Humanities, Nihon University, Tokyo 173-8610, Japan

[10]Innovative Therapy Research Group, Nihon University Research Institute of Medical Science, Tokyo 173-8610, Japan

Abstract

The MYC transcription factor plays a crucial role in the regulation of cell cycle progression, apoptosis, angiogenesis, and cellular transformation. Due to its oncogenic activities and over expression in a majority of human cancers, it is an interesting target for novel drug therapies. MYC binding to the E-box (5'-CACGTGT-3') sequence at gene promoters contributes to more than 4,000 MYC-dependent transcripts. Owing to its importance in MYC regulation, we designed a novel sequence-specific DNA-binding Pyrrole-Imidazole (PI) polyamide, Myc-5, that recognizes E-box consensus sequence. Bioinformatics analysis revealed that Myc-5 binding sequence appeared in 5′ MYC binding E-box sequences at the eIF4G1, CCND1 and CDK4 gene promoters. Furthermore Chromatin immunoprecipitation (ChIP) coupled with detection by qPCR demonstrated that Myc-5 has the ability to inhibit MYC-binding at the target gene promoters and thus cause down-regulation at m-RNA level and protein expression of its target gene in human Burkitt's lymphoma model cell line, P493.6, carrying an inducible MYC repression system and K562 (human chronic myelogenous leukaemia) cell lines. Single intravenous injection of Myc-5 at 7.5 mg/kg dose caused a significant tumor-growth inhibition in a MYC-dependent tumor xenograft model without evidence of toxicity. We report here a compelling rationale for the identification of a PI polyamide that inhibits a part of an E-box-mediated MYC downstream gene expression and is a model for showing that phenotype-associated MYC downstream gene targets consequently inhibits MYC dependent tumor growth.

Keywords

cell cycle; E-Box; MYC; pyrrole-imidazole polyamide; transcription therapy

Introduction

c-MYC is a transcription factor that possesses an exclusive and extensive set of biological actions that underlie its role as a salient oncogene and therefore could be the key to anticancer drug development. The c-MYC proto-oncogene belongs to the family of MYC genes that includes B-MYC, L-MYC, N-MYC, and S-MYC [(1)]. Among them c-MYC (here after referred as MYC) is found in almost all proliferating cells and expression of N- and L-MYC is more constrained to specific cell types [(2)]. MYC is a basics-helix–loop–helix leucine zipper (bHLH-LZ) transcription factor that binds DNA in a sequence-specific manner [(3)] and activates the transcription of genes whose products are involved in crucial aspects of cancer biology such as cell proliferation, cell growth, apoptosis and differentiation [(4)]. The biological activities of MYC depends on its ability to heterodimerize with its protein partner, MAX, to bind the Enhancer Box (E-box) sequence and stimulate transcription of a number of its downstream genes [(4;5)]. The MAX:MAX homodimer or

MAD:MAX heterodimer is supposed to antagonize the functions of MYC by binding to the same core E-box sequences [6].

MYC targets about 10–15% of all cellular promoters in human cells, which is higher than any other typical transcription factor [7]. Target genes of MYC identified in mammalian cells, include genes involved in cell cycle, ribosomal biogenesis, protein synthesis and mitochondrial function [4;5;8]. Among these direct target genes of MYC the one with E-box binding sites include ODC, ECA39, eIF4E, CDC25, CAD, CDK4, eIF4G1 and CCND1 genes [9;10]. MYC has been known to play crucial role in malignant transformation [11]. Several attempts have been made using small molecule inhibitors to inhibit MYC binding at gene promoters [11–16]. Pyrrole-imidazole (PI) polyamides are a class of sequence-specific DNA-binding small molecules that have been shown to be effective inhibitors of transcription factors by disrupting essential protein-DNA interactions [17–21]. Our group and others have designed PI polyamides to specifically target critical regulatory proteins, including MMP-9, TGF-β1, VEGF, HIF1-α, AR, EGFR, PSA, and LOX-1 [17;22–25]. Recently we have designed PI polyamides recognizing E-box, Myc-6 which significantly suppresses malignant phenotypes of human osteosarcoma MG63 cells both *in vitro* and *in vivo* showing potential of PI polyamide in cancer therapy [26].

In the present study, we developed an E-box binding PI polyamide, Myc-5 (target sequence; 5′-WCWCGWGW-3; where W= A or T) to inhibit MYC target genes. Myc-5 showed inhibition of MYC-driven cell-growth by down regulation of a subgroup of MYC downstream genes, including eIF4GI and CCND1 at early stage of transcription. In animal tumor model studies, Myc-5 inhibits tumor growth by inhibiting cell proliferation and inducing apoptosis in tumor tissue. Collectively, our results establish a transcriptional regulation at early stage of MYC regulatory proteins by using PI polyamides and provide a novel antitumor agent targeting MYC function.

Materials and Methods

Cell culture

The human Burkitt's lymphoma model cell line, P493.6, carrying Tet-repressible c-MYC system and chronic myeloid leukemia cell line K562, were used in this study. To suppress MYC expression P493.6 cells were treated with 0.1 μg/ml tetracycline for three days before treatment with Myc-5. P493.6 cell line were kindly provided by C. Grandori (FHRC, Seattle, Washington, USA) and K562 cells were obtained from the RIKEN cell bank (Ibaraki, Japan).

Synthesis of PI polyamides targeting the E-box consensus sequence

Myc-5 was designed to target the E-Box consensus sequence and mismatched PI polyamide was designed to target by exchanging CG dinucleotide with GC in the center of the E-box (Figs. 1A and 1C). Fluorescein isothiocyanate (FITC)-conjugated Myc-5 was also synthesized for nuclear localization experiments (Fig. 1B). All of the PI polyamides were synthesized according to previously established methods [22].

Electrophoretic mobility shift assay (EMSA) and Surface Plasmon Resonance (SPR)

FITC-labeled match 46 base pair hairpin oligonucleotide corresponding to eIF4G1 gene promoters having E-Box consensus binding sites and mismatch promoter were synthesized (Table S1) for EMSA. Results were visualized by luminescent image analyzer LAS3000 (Fuji film, Japan). The kinetic measurements of the polyamides binding curves to the biotin-labeled double-stranded DNA (having E-box consensus sequence) and data processing were performed on a Biacore 2000 system as described previously [(27)].

Quantitative real-time PCR (qPCR)

Total RNA was extracted and digested with DNaseI using the RNeasy kit according to manufacturer's protocol (QIAGEN). The primer sequences are listed in the Table S2. Relative gene expression was determined by normalizing the gene expression of each target gene to GAPDH.

qChIP (conventional ChIP followed by real-time PCR)

The status of polyamide binding at the target promoter region (Table S3) was detected using a ChIP assay kit (Upstate Biotechnology) following manufacturer protocol. ChIP DNA was further analyzed by qPCR using primers encompassing the regions of interest on the eIF4G1, CCND1 and CDK4 promoter.

Tumorigenicity studies in SCID mice

Seven weeks old SCID mice were housed under specific pathogen-free conditions. Experiments were approved by the committee for laboratory animal welfare and ethics of Nihon University School of Medicine, Tokyo, Japan. The effect of Myc-5 on the xenograft model was examined as follows: 1×10^7 P493.6 cells were inoculated subcutaneously (s.c.) in the flank of the mouse. The mice were divided into three groups: a control group of (PBS i.v.; n=8), a Myc-5–treated group of (7.5 mg/kg i.v., single dose; n=8), and a doxycycline treated group: 0.01% of doxycycline in regular drinking water (n=5). Doxycycline-induces repression of P493.6 xenograft tumor growth in MYC-dependent manner. The treatment was started on day seven after cell inoculation and mice were sacrificed after 30 days of treatment.

In vivo nuclear localization

For *in vivo* nuclear localization analysis by fluorescence microscopy, tumor-bearing mice were injected with FITC-labeled Myc-5 (0.15 mg) into the lateral tail vein of the animals. Tumor tissues, along with adjacent normal tissues were collected five days after the injection for analysis using propidium iodide as a nuclear dye to identify nucleated cells.

Statistical analysis

Results were shown as mean SD. Each experiment was performed independently thrice. The level of significance (*P* values ** <0.05 and *** <0.001) was determined using the Student's *t* test.

Additional supplementary material and method for cell viability assay, detection of nuclear localization by confocal microscopy, histopathology, western blot analysis, microarray analyses and references can be found in Doc S1 and Doc S2.

Results

Identification of MYC target genes that harbor Myc-5 consensus sequence

E-boxes are present in many genes, but not all are known to be direct transcriptional targets of MYC. Based on compilations by Fernandez et al. [28], we found that 105 genes harbors the Myc-5 binding site (WCWCGWGW) in their E-box consensus sequence (Table S4). These genes can be classified into a wide range of functional classes. Here we focused on genes related to translation and proliferation. Among the top ten MYC-regulated genes, proliferation genes (CDK4, CCND1) and translation (eIF4G1) gene. Selected genes have been well characterized by previous researchers and are also well known direct targets of MYC [10;29;30].

DNA-Binding affinity and specificity of designed Myc-5 PI polyamide

EMSA and SPR assay are used to determine the binding affinity and specificity of PI polyamide to its target DNA. EMSA results demonstrated that a clear mobility band shift was (Fig.2A and 2B) detected when Myc-5 was incubated with eIF4G1 gene promoter oligonucleotide, whereas no shift was detected for the mismatched PI polyamide (Fig. 2A, lane 4) or eIF4G1 mismatch gene promoter (Fig. 2A, lane 5) in which the core recognition sequence, CACGTG, was replaced by CAGCTG. Increasing concentrations of the Myc-5, but not of the mismatch PI polyamide, bind to the eIF4G1 promoter oligo (Fig. 2B, lanes 2–5), suggesting that Myc-5 can specifically bind to sequences of their target gene-promoters. To further confirm binding of the E-box to the target gene promoter, we did a biosensor-SPR assay to explore the interaction of Myc-5 with biotinylated hairpin duplexes having WCWCGWGW sequences (Fig. 2C). The kinetic profile of Myc-5 revealed a relatively fast “on-rate” and slow “off-rate” in binding with a K_D of $4.81\pm2.79 \times 10^{-8}$ M. The mismatched PI polyamide showed slow “on rate” and fast “off rate” with K_D was calculated at $5.1\pm0.54\times10^{-5}$. In summary, these results confirm that the presence of the E-box in the DNA sequence has a pronounced influence on the binding of Myc-5 and yields a 654-times-higher affinity than the mismatched PI polyamide (Figs. 2D, 2E and Table S5).

Myc-5 inhibited cell proliferation and localized into nucleus in P493.6 and K562 cell lines

P493.6 and K562 cells were incubated with different concentration (1–10 μM) of Myc-5 and mismatch PI polyamide and viability was determined at 24, 48, and 72 hours after treatment, respectively. As shown in Figs. S1A and S1B, cell viability was significantly reduced ($P<0.001$ versus control) in both cell lines treated with Myc-5 in a time- and concentration-dependent manner. Nuclear localization of Myc-5 was determined by FITC conjugated Myc-5 using laser confocal fluorescence microscopy. Green fluorescence indicates the presence of Myc-5, while red fluorescence depicts the cell nuclei, indicating that Myc-5 localizes into nucleus within two hours (Figs. S2A, S2C and S2D). On the other hand cells incubated with FITC solution (control) at same concentration do not localize into nucleus (Fig. S2B) in both cell lines.

Myc-5 attenuates MYC binding at the gene promoter causes down-regulation of MYC target genes

Myc-5 inhibited target gene expression at protein and m-RNA levels (Fig. 3A & 3B). Cells treated with Myc-5 at 10μM concentration for 72 hours caused statistically significant suppression of eIF4G1 mRNA as compared with control or mismatched PI polyamide treated cells in both systems. The CCND1 m-RNA was unaffected in the all treated and untreated groups of P493.6 cells; however, its expression was significantly ($P < 0.001$) down-regulated in the K562 cell line compared to control and mismatch PI polyamide treated group. The mRNA expression correlated well with protein expression in the Myc-5 administration using both cell systems (Fig. 3C &D). To investigate whether target genes expression are directly regulated by Myc-5, we did ChIP assays of E-box and the Exonic region (Figs. 4A, 4B and Fig S3A). The Exonic region is taken as arbitrary negative control region as during the analysis. ChIP analysis revealed that compared to control Myc-5 and tetracycline group significantly inhibits binding of MYC to E-Box region in P493.6 cell (Fig. 4C and Fig S3B) at the eIF4G1 and CDK4 gene promoters. In contrast E-box and control region (Exon) of CCND1 gene promoter showed restrained enrichment in all treated groups (Fig. 4D). Similarly, MYC was specifically enriched near the E-box site at the eIF4G1, CCND1 and CDK4 gene promoters but not Myc-5 treated group in K562 cells (Figs. 4E, 4F and Fig S3C). Moreover our microarray analysis results showed (Supplementary Figs. S4A and S4B) that differentially expressed genes in K562 cells (29 up-regulated and 21 down-regulated), in P943.6 cells (20 genes up-regulated and 20 down-regulated) were identified by unpaired two-class Significance Analysis of Microarray (SAM) analysis with 0% False Discovery Rate (FDR). Among top 50 modulated genes, five genes were carrying Myc-5 consensus sequence in their promoter as identified from Supplementary Table S4.

Myc-5 administration retards growth in animal tumor models

To investigate if the *in vitro* efficacy of Myc-5 can also be recapitulated in vivo, therapeutic animal studies were conducted using P493.6 subcutaneous xenografts. Mice were inoculated s.c. with P493.6 (high MYC expressing) cells. At one week after inoculating the cells, when the tumor volumes reached around 100 mm^3, mice were split into three groups and treated with either saline, doxycycline or 7.5 mg/kg Myc-5 injected intravenously into the lateral tail vein animals at day 7 (single dose; Figure 5A). Myc-5 was formulated based on previous xenograft studies with PI polyamide [21;31;32]. Growth curve data indicated that Myc-5 (7.5 mg/kg) and doxycycline treated groups had a significantly smaller in tumor volume during the growth phase ($P<0.001$ versus control; Fig. 5B) by the end of study. Representative image of each group mice is shown in Fig 5B (inset). All mice with Myc-5 treatment continued to gain weight at an equal rate throughout the treatment period (Fig. 5D). The average tumor weight result further confirmed inhibition of tumor growth as Myc-5 and doxycycline treated groups were found to be significantly lower ($P < 0.001$ versus control; Fig 5E) at the termination of study.

Myc-5 localizes into the tumor and causes decreased cell proliferation and induced apoptosis in P493.6 tumor xenografts

To evaluate *in vivo* nuclear localization single intravenous injection of FITC-conjugated Myc-5 was given to P493.6 cell-derived xenograft. Twenty-four hours after intravenous injection of FITC-conjugated Myc-5 to xenografts, animals were killed and tumor tissues were obtained. The tumor-derived tissues were found to display strong and characteristic nuclear staining (Fig. 5C). In contrast, adjacent normal tissues found to be devoid of nuclear fluorescence (Fig. 5C). Myc-5 was found throughout the tumor, demonstrating its capacity of enter the tumor through the vascular system. To assess the activity of Myc-5, tumors were harvested from all treatment groups and examined by histopathology. Microscopic analysis of H&E staining showed that Myc-5 and doxycycline treated tumors exhibited areas with necrosis, cellular debris and swollen cells with cytoplasmic vacuoles as compared with the vehicle-treated control (Fig. 6A; left). In order to investigate the mechanism underlying Myc-5-mediated tumor growth inhibition in P493.6 xenografts, immunohistochemical analyses were conducted for BrdU uptake, and TUNEL reaction assay. BrdU-positive nuclei were detected in a small number of cells in Myc-5 treated tumor as compared to control group (Fig 6A; middle). In contrast a large number of cells stained positively for TUNEL in Myc-5 or Doxycycline treated group (Fig. 6A; left) compare to control group. Quantitative data were consistent with expression pattern of BrdU and TUNEL staining assays (Fig. 6B). Quantification of BrdU positive cells in control group were significantly ($P<0.001$) reduced (~83% and ~76% reduction in Myc-5 and doxycycline respectively) compared to treated groups. TUNEL analysis showed that number of apoptotic cells was significantly higher ($P<0.001$; ~38% and ~30% higher in Myc-5 and doxycycline respectively) in treated groups. Overall we found that Myc-5 is well tolerated, inhibits tumor growth and induces apoptosis in P493.6 xenograft mouse models.

Discussion

In this study we synthesized two β-alanine-linked polyamides of different lengths, Myc-5 (AcPyPyPyImβImγPyβPyImβImβDp), where Py is pyrrole, Im is imidazole, Ac is acetyl, β is β-alanine, Dp is dimethylaminopropylamine and γ is γ-*turn* to target the 8-bp site of 5′-WCWCGWGW-3′ and mismatched polyamide (AcPyβImPyPyImγPyPyImPyβImβDp) to target the 8-bp site 5′-WCWGCWGW-3′ flipping dinucleotides of CG to GC at the central portion (Figs. 1A, 1B). A search for Myc-5-binding sites from the published database [28] revealed that the Myc-5 consensus sequence was flanking to a E-box of genes involved in apoptosis, cell cycle, nucleolar function, ribosomal proteins and translation initiation factors. Among them, we focused on the eIF4G1, CCND1 and CDK4 genes because they carry a Myc-5 consensus sequence including a MYC binding site (E-box) in the promoter region (Fig S3D) and their transcription are modulated by MYC [9;10;30]. Using EMSA and Biacore analyses, our results demonstrated that Myc-5 binds specifically and with high affinity (654 times; Table S5) to the eIF4G1, CCND1 and CDK4 gene promoter at E-box region (Fig. 2). The effective concentration of Myc-5 in the EMSA was higher than the concentration for biological effect, which is consistent with results obtained for other compounds [33]; possibly, PI polyamide accumulates in cells to effectively reach the intracellular and intra-nuclear levels [34]. The higher binding affinity of Myc-5 in comparison to mismatch PI

polyamide might be explained as the targeted PI polyamide has more aliphatic β-alanine unit giving it more flexibility and optimizes the positioning of the imidazole amino acids on binding to its targeted sequence [35]. *In vivo* binding of Myc-5 to their target gene-promoter was confirmed by ChIP assay. Results of ChIP demonstrated that MYC transcription factor binds E-box in control group whereas in treated group Myc-5 inhibits MYC binding on its target gene promoters. However in the P493.6 cell lines the CCND1 gene-promoter showed only background signal that was obtained at the E-box region as well as in the control (Exon) regions (Fig. 4D). These results were consistent with previous studies reports of the absence of this regulator in the B cells line [36].

Myc-5 is used at the concentration of 10 μM based on previous studies using PI polyamides [38–40]. Myc-5 significantly reduced m-RNA and protein expression of MYC target genes at this given concentration. The correlation between the MYC binding and m-RNA expression of Myc-5 was established by real-time m-RNA expression analysis and western blot analysis. The eIF4G1 gene has a down-regulated expression and might be a direct target of MYC in both systems, which was also favored by EMSA and ChIP data. CCND1 m-RNA expression was down-regulated in the K562 cell line with Myc-5 treatment in a dose-dependent manner, which is known to exert positive growth effects and to be regulated by MYC [37]. The m-RNA expression of *CDK4*, a positive growth controller of MYC [30], was unaffected by Myc-5 treated group as Myc-5 binding site (E Box#2) has no role in MYC dependent gene regulation (30). We analyzed the CDK4 promoter region for putative MYC binding sites. Our sequence analysis revealed the presence of four E-box sequences, which could be recognized by MYC (Figure S2). Among them only E-box#2 is a putative binding site for Myc-5 as it contains Myc-5 consensus sequence. As shown in Figure S2, Myc-5 bound to the E-box#2 of the CDK4 promoter. CDK4 gene is established as direct target of MYC identified by serial analysis of gene expression with essential E boxes in their promoters [30]. The CDK4 promoter contains four highly conserved E-box elements where E box#3 and #4 were the most important for CDK4 promoter activity [30]. Effect of Myc-5 on m-RNA expression on the MYC gene and further its transcriptional target CDK4 gene by real time PCR in K562 and P493.6 cell lines. In K562 cell MYC m-RNA expression is unaffected by Myc-5 treatment and similar trend was observed in its target gene CDK4 m-RNA expression. On the other hand in P493-6 B lymphoma cells cultured with (MYC-off) or without (MYC-on) tetracycline. P493.6 cells, MYC m-RNA expression is induced by Myc-5 treatment with respect to control group. P493.6 B lymphoma cells are MYC over expressing cell line which indicates P493.6 cell lines may have some mutations on its promoter or regulator regions. MYC promoter or regulatory region in do not have any Myc-5 binding consensus sequence. May be due to some specific mutation in the MYC promoter or regulatory regions of have generated a novel Myc-5 binding site at the MYC promoter of P493.6 cells. This novel Myc-5 binding site in the promoter is acting as a transcriptional activator of the MYC gene and helping it to further over express. Furthermore, Myc-5 has very high affinity for its consensus sequence and may be act as a non-competitive inhibitor of MYC protein. Therefore, over expression MYC protein in P493.6 cells does not have an effect on MYC downstream genes with active Myc-5 binding site such a eIF4G1.

Taken together, our data are compatible with a mechanism that involves the recruitment of Myc-5 at E-Box sites within the promoter of the MYC target gene thereby inhibiting MYC binding at particular site and inhibits target gene function instead blocking MYC. Myc-5 down-regulates its target gene transcription supporting the notation that polyamides bind to DNA with affinity and sequence-specificity comparable to DNA-binding proteins and gene expression can be regulated by competitive displacement of transcription factor from DNA target sequences [(41)], where Myc-5 consensus sequences are not contained.

Myc-5 exerts its therapeutic role in tumor maintenance via selective effects on the translation of specific downstream genes. In our *in vivo* study we have used 7.5 mg/kg on the basis of prior pharmacokinetic profile and previous analytical studies [(38;42)]. We identified the strong *in vivo* nuclear localization of Myc-5 and also inhibitory effect on the tumor growth in P493.6 mouse model. One possible reason of this activity can be explained by previous reports showing that changes in the levels or activity of eIF4F mediate the translational regulation of specific genes involved (as in P493.6 cell line eIF4G1 is completely suppressed) in survival and apoptosis [(43)]. In nasopharyngeal carcinoma, knockdown of eIF4G1 expression markedly inhibited cell-cycle progression, proliferation, and suppressed *in vivo* xenograft tumor growth [(44;45)], which might be applicable to our system as well.

In conclusion, the results reported here identify a novel PI polyamide, Myc-5 as a lead compound targeting against the E-box and thereby modulating expression of some genes. Our approach can be an efficient tool to identify the sequence-specific compound that targets the E-box and specifically modulates MYC downstream genes and interfere with their pathway. Myc-5 competes with the MYC: MAX heterodimer and inhibit trans-regulation of the target gene promoter (Fig. 6D) at the E-Box. However, the extension of this approach could result in the identification of more potent inhibitory PI polyamides in multiple pathways and reveal a new E-box-regulated target or combination of targets for a distinct MYC function, which may have formidable therapeutic opportunities for the future.

Supplementary Material

Refer to Web version on PubMed Central for supplementary material.

Aknowledegement

We thank Mr. Shigeki Nakai, Ms. Asako Oguni, Mr. Motoaki Kataba, Ms. Yuki Yamada and Ms. Yukari Obana, for their technical support and Ms. Paula Jones, Dr. Manisha Tripathi and Dr. Sandrine Billet for critical reading.

Financial support: This work is supported by the Academic Frontier Project for 2006 Project for Private Universities, a matching fund subsidy and Grant-in-Aid for Scientific Research (B) #23300344 and # 26290060 from the Ministry of Education, Culture, Sports, Science and Technology to H. Nagase. The Setsuro Fujii Memorial, the Osaka Foundation for the Promotion of Fundamental Medical Research to H. Nagase. The Nihon University Strategic Projects for Academic Research and R01 ES012249 from National Institute of Health (NIH)/ National Institute of Environmental Health Science (NIEHS) to H. Nagase.

Reference List

1. Adhikary S, Eilers M. Transcriptional regulation and transformation by Myc proteins. Nat Rev Mol Cell Biol. 2005; 6:635–645. [PubMed: 16064138]

2. Luscher B. Function and regulation of the transcription factors of the Myc/Max/Mad network. Gene. 2001; 277:1–14. [PubMed: 11602341]
3. Blackwood EM, Eisenman RN. Max: a helix-loop-helix zipper protein that forms a sequence-specific DNA-binding complex with Myc. Science. 1991; 251:1211–1217. [PubMed: 2006410]
4. Dang CV, O'Donnell KA, Zeller KI, et al. The c-Myc target gene network. Semin Cancer Biol. 2006; 16:253–264. [PubMed: 16904903]
5. Liu YC, Li F, Handler J, et al. Global regulation of nucleotide biosynthetic genes by c-Myc. PLoS One. 2008; 3:e2722. [PubMed: 18628958]
6. Ayer DE, Eisenman RN. A switch from Myc:Max to Mad:Max heterocomplexes accompanies monocyte/macrophage differentiation. Genes Dev. 1993; 7:2110–2119. [PubMed: 8224841]
7. Guccione E, Martinato F, Finocchiaro G, et al. Myc-binding-site recognition in the human genome is determined by chromatin context. Nat Cell Biol. 2006; 8:764–770. [PubMed: 16767079]
8. Zeller KI, Jegga AG, Aronow BJ, et al. An integrated database of genes responsive to the Myc oncogenic transcription factor: identification of direct genomic targets. Genome Biol. 2003; 4:R69. [PubMed: 14519204]
9. Huerta M, Munoz R, Tapia R, et al. Cyclin D1 is transcriptionally down-regulated by ZO-2 via an E box and the transcription factor c-Myc. Mol Biol Cell. 2007; 18:4826–4836. [PubMed: 17881732]
10. Lin CJ, Cencic R, Mills JR, et al. c-Myc and eIF4F are components of a feedforward loop that links transcription and translation. Cancer Res. 2008; 68:5326–5334. [PubMed: 18593934]
11. Albihn A, Johnsen JI, Henriksson MA. MYC in oncogenesis and as a target for cancer therapies. Adv Cancer Res. 2010; 107:163–224. [PubMed: 20399964]
12. Wang H, Chauhan J, Hu A, et al. Disruption of Myc-Max heterodimerization with improved cell-penetrating analogs of the small molecule 10074-G5. Oncotarget. 2013; 4:936–947. [PubMed: 23801058]
13. Wang H, Hammoudeh DI, Follis AV, et al. Improved low molecular weight Myc-Max inhibitors. Mol Cancer Ther. 2007; 6:2399–2408. [PubMed: 17876039]
14. Yin X, Giap C, Lazo JS, et al. Low molecular weight inhibitors of Myc-Max interaction and function. Oncogene. 2003; 22:6151–6159. [PubMed: 13679853]
15. Delmore JE, Issa GC, Lemieux ME, et al. BET bromodomain inhibition as a therapeutic strategy to target c-Myc. Cell. 2011; 146:904–917. [PubMed: 21889194]
16. Yin X, Giap C, Lazo JS, et al. Low molecular weight inhibitors of Myc-Max interaction and function. Oncogene. 2003; 22:6151–6159. [PubMed: 13679853]
17. Dervan PB, Doss RM, Marques MA. Programmable DNA binding oligomers for control of transcription. Curr Med Chem Anticancer Agents. 2005; 5:373–387. [PubMed: 16101489]
18. Dickinson LA, Burnett R, Melander C, et al. Arresting cancer proliferation by small-molecule gene regulation. Chem Biol. 2004; 11:1583–1594. [PubMed: 15556009]
19. Nickols NG, Szablowski JO, Hargrove AE, et al. Activity of a py-im polyamide targeted to the estrogen response element. Mol Cancer Ther. 2013; 12:675–684. [PubMed: 23443804]
20. Yang F, Nickols NG, Li BC, et al. Antitumor activity of a pyrrole-imidazole polyamide. Proc Natl Acad Sci U S A. 2013; 110:1863–1868. [PubMed: 23319609]
21. Raskatov JA, Nickols NG, Hargrove AE, et al. Gene expression changes in a tumor xenograft by a pyrrole-imidazole polyamide. Proc Natl Acad Sci U S A. 2012; 109:16041–16045. [PubMed: 22988074]
22. Wang X, Nagase H, Watanabe T, et al. Inhibition of MMP-9 transcription and suppression of tumor metastasis by pyrrole-imidazole polyamide. Cancer Sci. 2010; 101:759–766. [PubMed: 20085585]
23. Nickols NG, Jacobs CS, Farkas ME, et al. Modulating hypoxia-inducible transcription by disrupting the HIF-1-DNA interface. ACS Chem Biol. 2007; 2:561–571. [PubMed: 17708671]
24. Matsuda H, Fukuda N, Ueno T, et al. Transcriptional inhibition of progressive renal disease by gene silencing pyrrole-imidazole polyamide targeting of the transforming growth factor-beta1 promoter. Kidney Int. 2011; 79:46–56. [PubMed: 20861821]
25. Kang JS, Meier JL, Dervan PB. Design of sequence-specific DNA binding molecules for DNA methyltransferase inhibition. J Am Chem Soc. 2014; 136:3687–3694. [PubMed: 24502234]

26. Taniguchi M, Fujiwara K, Nakai Y, et al. Inhibition of malignant phenotypes of human osteosarcoma cells by a gene silencer, a pyrrole-imidazole polyamide, which targets an E-box motif. FEBS Open Bio. 2014; 4:328–334.
27. Chen M, Matsuda H, Wang L, et al. Pretranscriptional regulation of Tgf-beta1 by PI polyamide prevents scarring and accelerates wound healing of the cornea after exposure to alkali. Mol Ther. 2010; 18:519–527. [PubMed: 19920805]
28. Fernandez PC, Frank SR, Wang L, et al. Genomic targets of the human c-Myc protein. Genes Dev. 2003; 17:1115–1129. [PubMed: 12695333]
29. Huerta M, Munoz R, Tapia R, et al. Cyclin D1 is transcriptionally down-regulated by ZO-2 via an E box and the transcription factor c-Myc. Mol Biol Cell. 2007; 18:4826–4836. [PubMed: 17881732]
30. Hermeking H, Rago C, Schuhmacher M, et al. Identification of CDK4 as a target of c-MYC. Proc Natl Acad Sci U S A. 2000; 97:2229–2234. [PubMed: 10688915]
31. Chou CJ, Farkas ME, Tsai SM, et al. Small molecules targeting histone H4 as potential therapeutics for chronic myelogenous leukemia. Mol Cancer Ther. 2008; 7:769–778. [PubMed: 18413791]
32. Chou CJ, O'Hare T, Lefebvre S, et al. Growth arrest of BCR-ABL positive cells with a sequence-specific polyamide-chlorambucil conjugate. PLoS One. 2008; 3:e3593. [PubMed: 18974832]
33. Berg T, Cohen SB, Desharnais J, et al. Small-molecule antagonists of Myc/Max dimerization inhibit Myc-induced transformation of chicken embryo fibroblasts. Proc Natl Acad Sci U S A. 2002; 99:3830–3835. [PubMed: 11891322]
34. Yao EH, Fukuda N, Ueno T, et al. A pyrrole-imidazole polyamide targeting transforming growth factor-beta1 inhibits restenosis and preserves endothelialization in the injured artery. Cardiovasc Res. 2009; 81:797–804. [PubMed: 19098300]
35. Farkas ME, Li BC, Dose C, et al. DNA sequence selectivity of hairpin polyamide turn units. Bioorg Med Chem Lett. 2009; 19:3919–3923. [PubMed: 19349175]
36. Arvanitakis L, Yaseen N, Sharma S. Latent membrane protein-1 induces cyclin D2 expression, pRb hyperphosphorylation, and loss of TGF-beta 1-mediated growth inhibition in EBV-positive B cells. J Immunol. 1995; 155:1047–1056. [PubMed: 7636179]
37. Mateyak MK, Obaya AJ, Sedivy JM. c-Myc regulates cyclin D-Cdk4 and -Cdk6 activity but affects cell cycle progression at multiple independent points. Mol Cell Biol. 1999; 19:4672–4683. [PubMed: 10373516]
38. Raskatov JA, Nickols NG, Hargrove AE, et al. Gene expression changes in a tumor xenograft by a pyrrole-imidazole polyamide. Proc Natl Acad Sci U S A. 2012; 109:16041–16045. [PubMed: 22988074]
39. Wang YD, Dziegielewski J, Wurtz NR, et al. DNA crosslinking and biological activity of a hairpin polyamide-chlorambucil conjugate. Nucleic Acids Res. 2003; 31:1208–1215. [PubMed: 12582240]
40. Yang F, Nickols NG, Li BC, et al. Antitumor activity of a pyrrole-imidazole polyamide. Proc Natl Acad Sci U S A. 2013; 110:1863–1868. [PubMed: 23319609]
41. Nickols NG, Dervan PB. Suppression of androgen receptor-mediated gene expression by a sequence-specific DNA-binding polyamide. Proc Natl Acad Sci U S A. 2007; 104:10418–10423. [PubMed: 17566103]
42. Synold TW, Xi B, Wu J, et al. Single-dose pharmacokinetic and toxicity analysis of pyrrole-imidazole polyamides in mice. Cancer Chemother Pharmacol. 2012; 70:617–625. [PubMed: 22907527]
43. Li S, Perlman DM, Peterson MS, et al. Translation initiation factor 4E blocks endoplasmic reticulum-mediated apoptosis. J Biol Chem. 2004; 279:21312–21317. [PubMed: 14990584]
44. Tu L, Liu Z, He X, et al. Over-expression of eukaryotic translation initiation factor 4 gamma 1 correlates with tumor progression and poor prognosis in nasopharyngeal carcinoma. Mol Cancer. 2010; 9:78. [PubMed: 20398343]
45. Lin CJ, Nasr Z, Premsrirut PK, et al. Targeting synthetic lethal interactions between Myc and the eIF4F complex impedes tumorigenesis. Cell Rep. 2012; 1:325–333. [PubMed: 22573234]

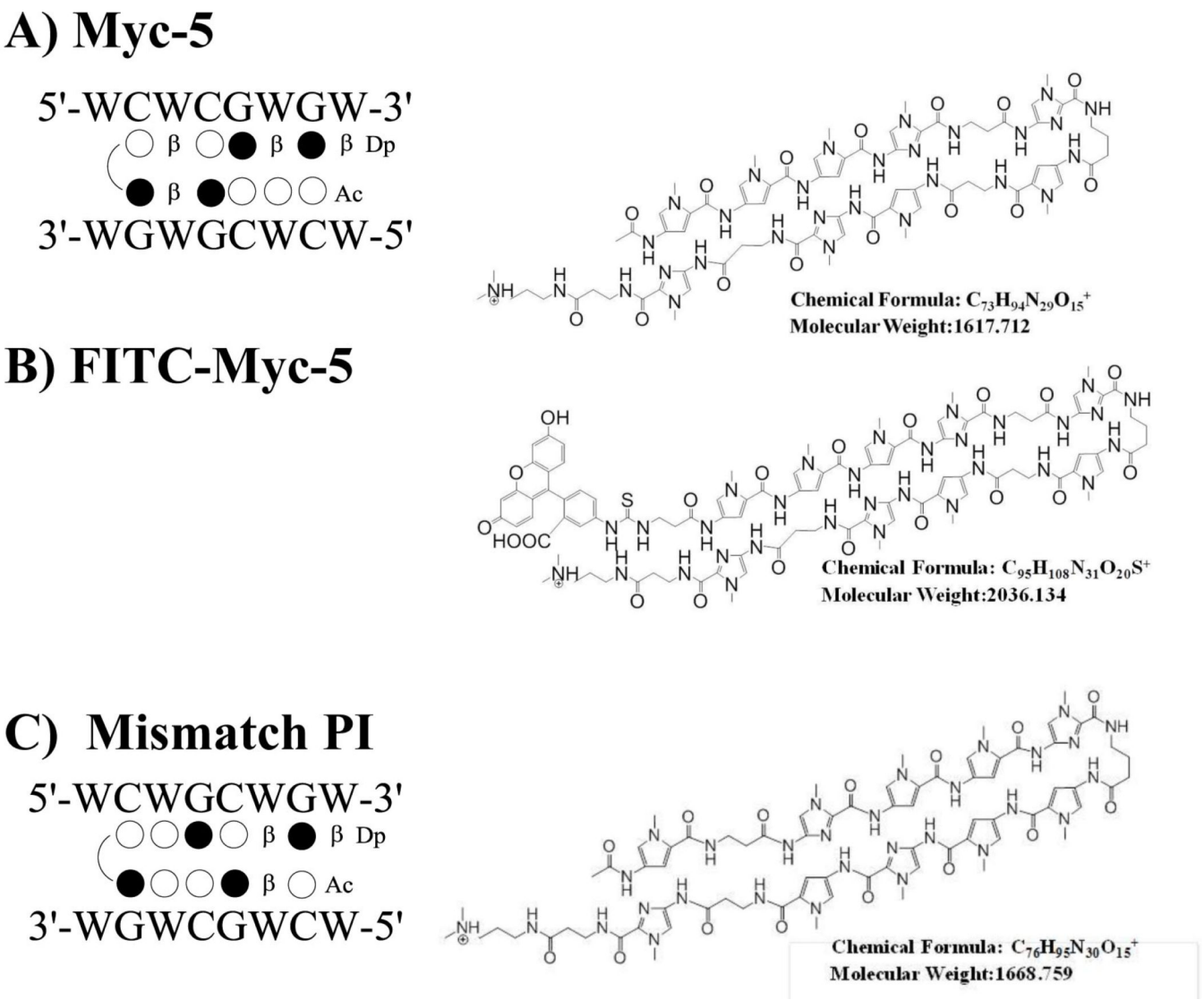

Figure 1. Designed PI polyamide structure and binding site

Structures and binding sites for synthesized PI polyamides ***A***, Myc-5; ***B***, FITC labeled Myc-5 ***C***, Mismatch PI polyamide. Base sequence specificity depends on side-by-side pairing of Pyrrole and Imidazole amino acids in the minor groove of DNA. Black and white circles, Im and Py rings, respectively; curved line, hairpin junction,; β is β-alanine; Dp is diaminomethylene propylamide and W=A or T.

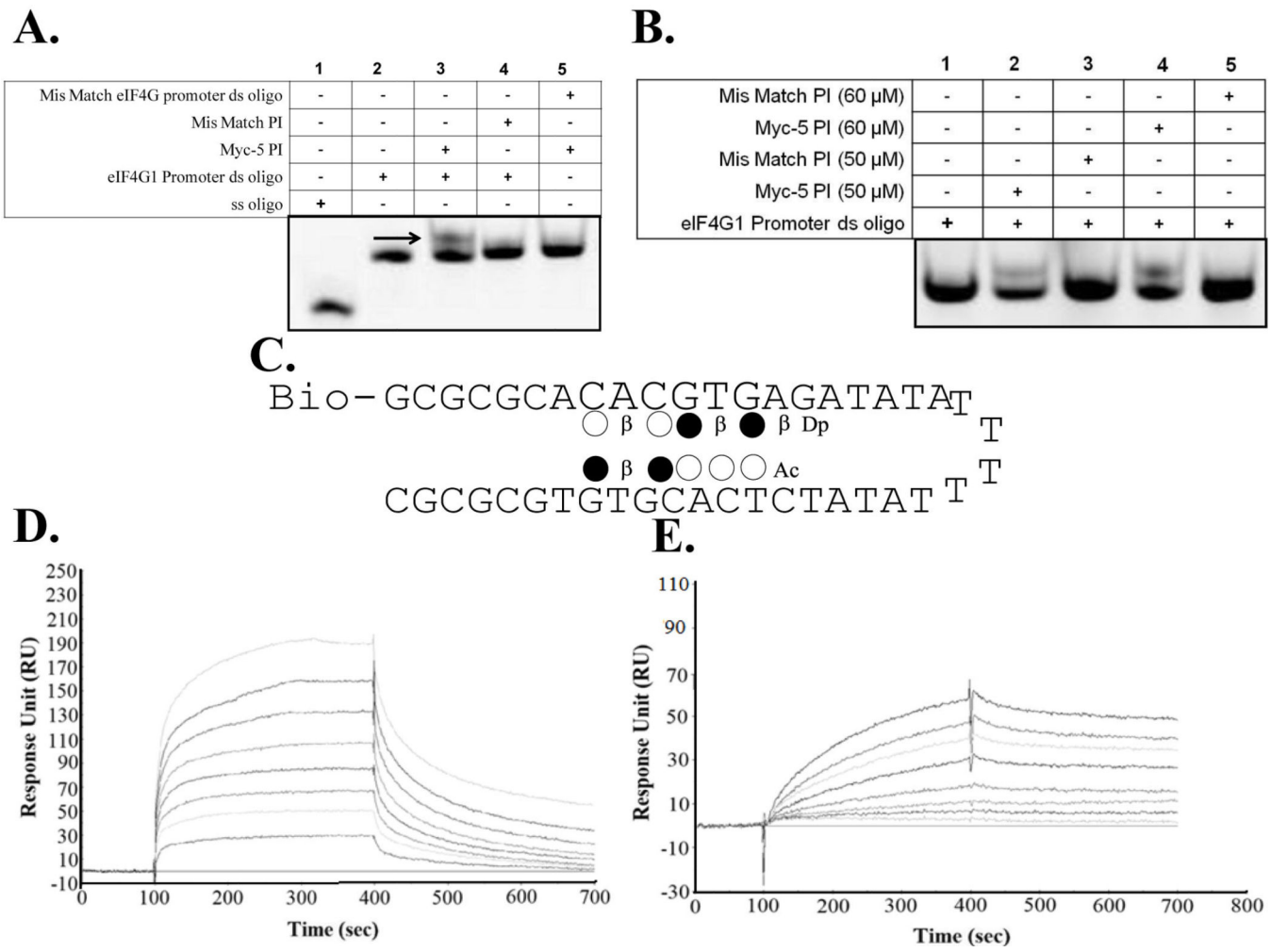

Figure 2. Myc-5 binding at the target gene promoters

A, EMSA of eIF4G1 gene match and mismatch promoter and with Myc-5 and mismatched PI polyamide. ***B***, EMSA of eIF4G1 gene promoter with Myc-5 and mismatched PI polyamide. FITC-labeled hairpin oligonucleotide was incubated at 37°C for 60 min in Myc-5 or mismatched PI polyamide. ***C***, Typical SPR sensograms for the interaction of PI polyamides with the hairpin duplex with 5'-biotin labeled and immobilized E-box (CACGTG) sequences. ***D–E***, Remarkable differences in binding kinetics are observed: fast on/off kinetics for Myc-5 (D) and slower kinetics for the mismatch PI polyamide (E).

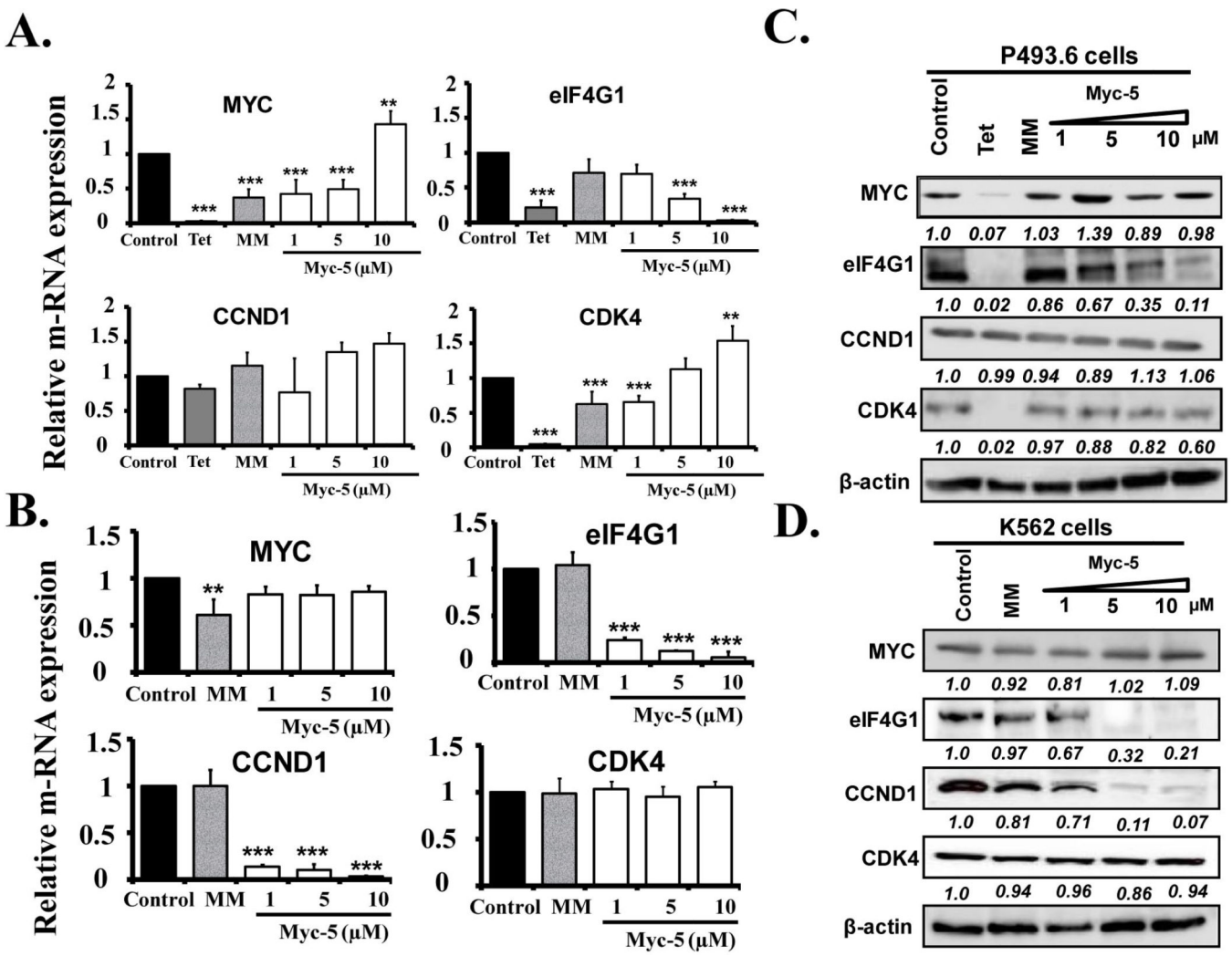

Figure 3. Myc-5 down-regulates m-RNA expression and protein expression of the target genes

A-B, Gene expression of target gens were detected by quantitative real time PCR after 72 hour of control and treated with Myc-5 (1,5 and 10 μM conc.) and mismatch PI polyamide (MM) at 10 μM conc. and normalized with GAPDH in (A) P493.6 and (B) K562 cells. The data in A and B are shown as mean value with error bars representing ± SD. Statistical significance was calculated by Student's t test. **, $p<0.05$, **, $p<0.001$ when compared to control. C-D, P493.6 and K562 cells were treated with Myc-5 (1, 5 and 10 μM) and mismatch PI polyamide (10 μM) for 72 hours. Western blotting was performed as described in supplementary material method section. β-actin was used at loading control. The Relative band intensities in P493.6 and K562 cells was determined by dividing the intensity of the band by β-actin followed by normalization to the control.

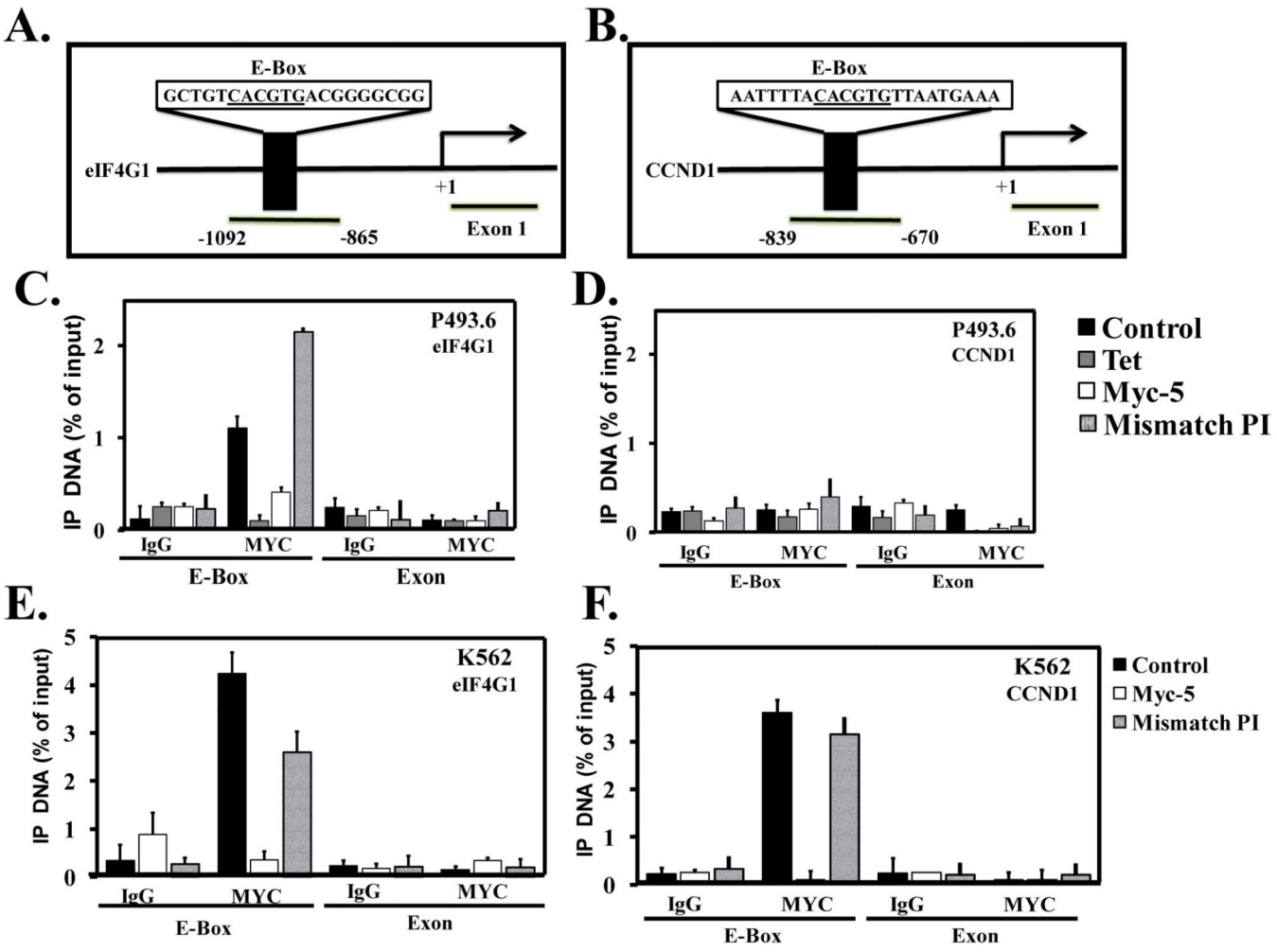

Figure 4. ***In vivo*** **binding of Myc-5 to the E-box at its target gene promoter**

A-B, Schematic depiction of the Myc-5 target gene promoter with MYC binding site (underline) indicated. ***C–D***, ChIP assay of Myc-5 target genes in the P493.6 and ***E–F***, K562 cell system. Labeled regions (E-box and Exon) of each gene were quantitatively amplified by real-time PCR. Data are representative of three independent experiments.

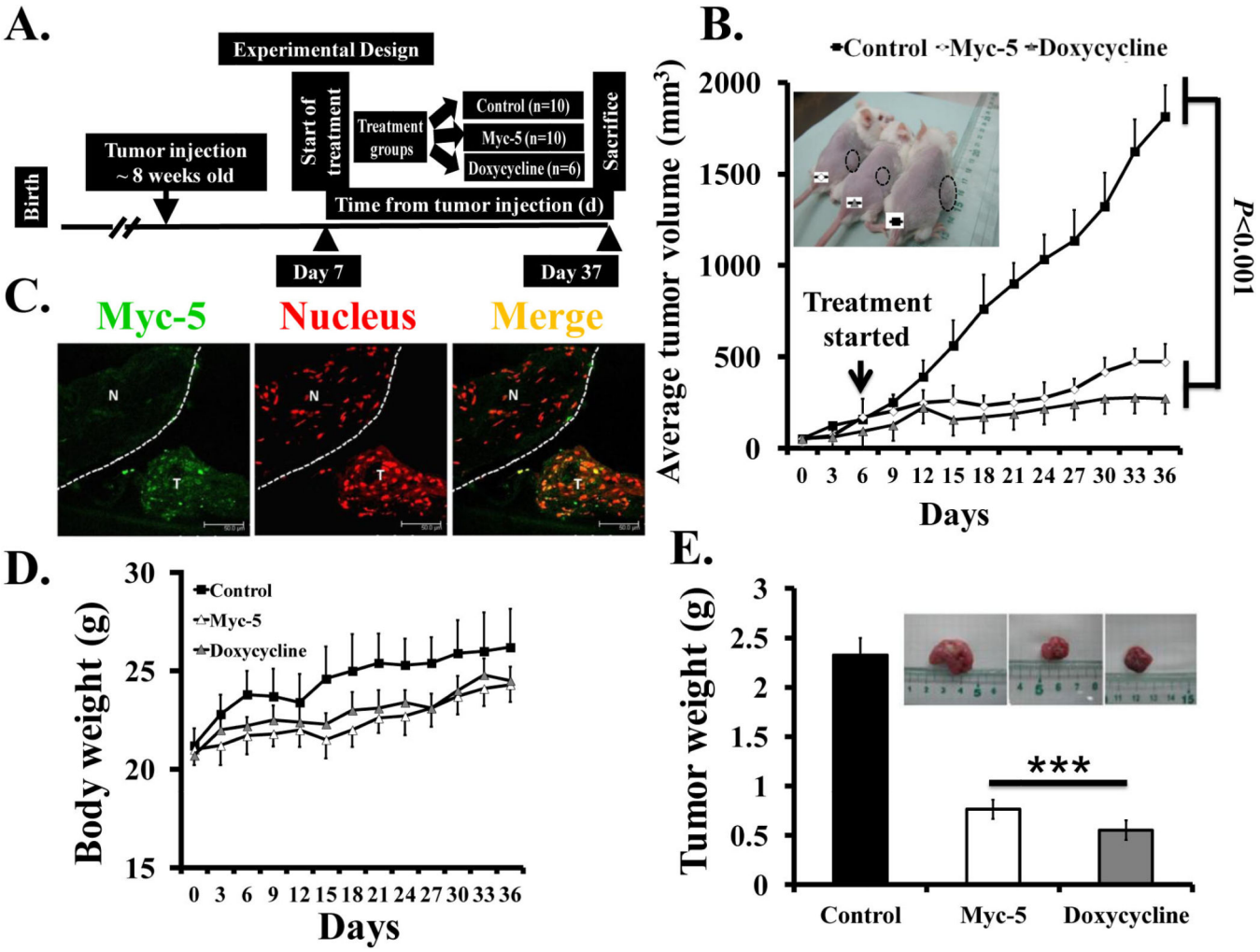

Figure 5. Myc-5 blocks the growth of P493.6 xenografts

A, Schematic diagram of the xenograft model illustrating timing of tumor implantation and treatment. Eight weeks old SCID mice were subcutaneously injected with P493.6 cells. ***B***, Tumor-growth chart showing the effect of treatment *in vivo*. Myc-5 (7.5 mg/kg) and doxycycline significantly slowed tumor growth ($P<0.001$) at termination point in comparison to control group. Representative picture of each group mice (inset). ***C***, FITC-labeled Myc-5 localizes to nucleus of P493.6 xenograft leaving normal tissue unaffected (separated by white line). N: Normal tissue, T: tumor tissue. ***D***, Mean body-weight for each treatment group plotted as function of day after post-injection. ***E***, Comparisons of excised tumor weights for three different treatment groups at the end of study are shown. The data in B, D and E are shown as the mean ± SD. Statistical significance was calculated by Student's t test. ***P < 0.001.

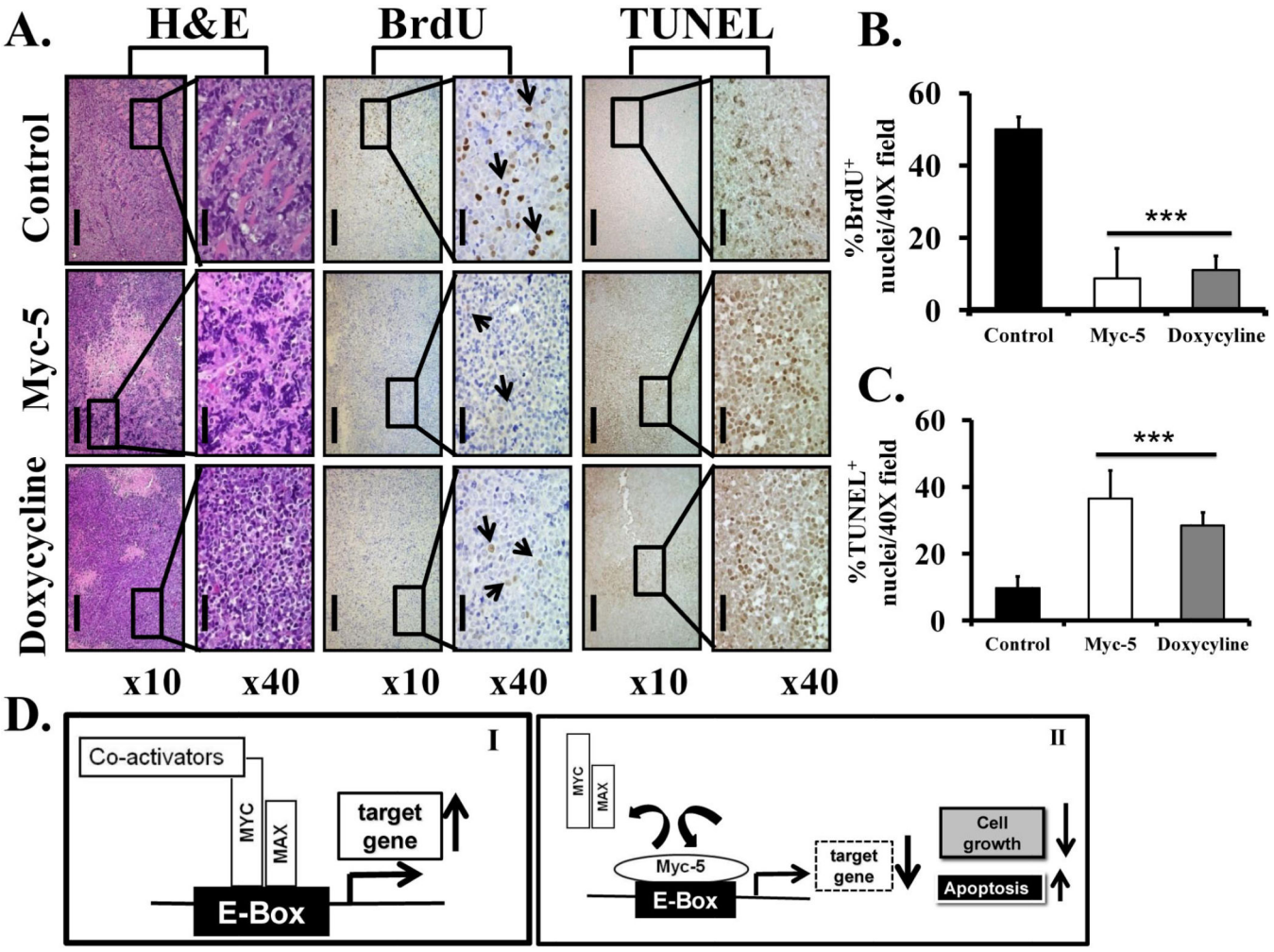

Figure 6. Histopathology of xenografts in nude mice and illustration of potential mechanism by Myc-5

A, Tissue sample were analyzed qualitatively for the morphological changes. Magnification of all pictures is ×10 (scale bar 200μm) and ×40 magnification (scale bar 50μm). ***B–C***, Quantitative data of immunohistochemical analysis of BrdU and TUNEL positive staining in each group. The data in B and C are shown as the mean ± SD of three tumor samples from an individual mouse in each group.. Statistical significance was calculated by Student's t test. ***P < 0.001. ***D***, Schematic diagram of the mechanism by which PI polyamide inhibits MYC/MAX interaction to E Box. (I), MYC/MAX dimer binds to E-box and activates MYC target gene expression. (II), Myc-5 occupied the E-box by binding, thereby inhibiting the MYC/MAX interaction to E-box further causing suppression of target gene expression.